ASIA TURBOMACHINERY & PUMP SYMPOSIUM
MARCH 2018 | SUNTEC SINGAPORE

Operating Conditions of Floating Ring Annular Seals

Mihai ARGHIR
Institut PPRIME, UPR CNRS 3346, Université de Poitiers, ISAE ENSMA, France
Antoine MARIOT
Safran Aircraft Engines, France

Authors Bio

Mihai ARGHIR is Professor at Université de Poitiers in France. His main research interests are in lubricated bearings and seals mainly used by the aeronautical and aerospace industry. Dr. Arghir authored more than 50 papers in archival journals and is Fellow of the ASME.

Antoine MARIOT has an engineer degree from Ecole d'Art et Métiers in France and got his PhD from the Université de Poitiers in 2015. He is now a R&D engineer at Safran Aircraft Engines in Villaroche, France. He specializes in various types of dynamic sealing systems used in turbine engines and is in charge of R&D projects for future engine programs.

Example: a buffer seal made of two FRAS

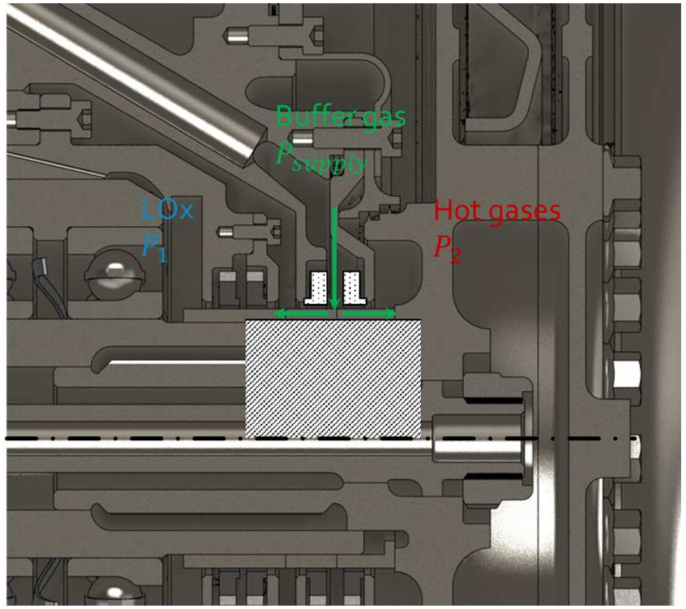

- A “buffer” gas (N_2, He…) is injected between 2 seals in a back-to-back configuration
- $P_{supply} > P_1, P_2$
- $\Delta P = P_{supply} - P_i$
- The buffer gas creates a barrier between the two sides of the machine
- Additional seals may be used to lessen P_1, P_2 in order to reduce the required P_{supply}

General description of the floating ring annular seal

- The carbon ring is mounted in a steel collar
- The main seal is a small radial clearance between the annular faces (≈ 25 µm)
- The pressure difference $\Delta P = P_{upstr} - P_{downstr}$ presses the “nose” of the floating ring against the stator and creates the secondary seal
- The ring “floats” on the rotor and follows rotor vibrations
- It allows large rotor excursions without using a large clearance annular seal and therefore has a limited leakage

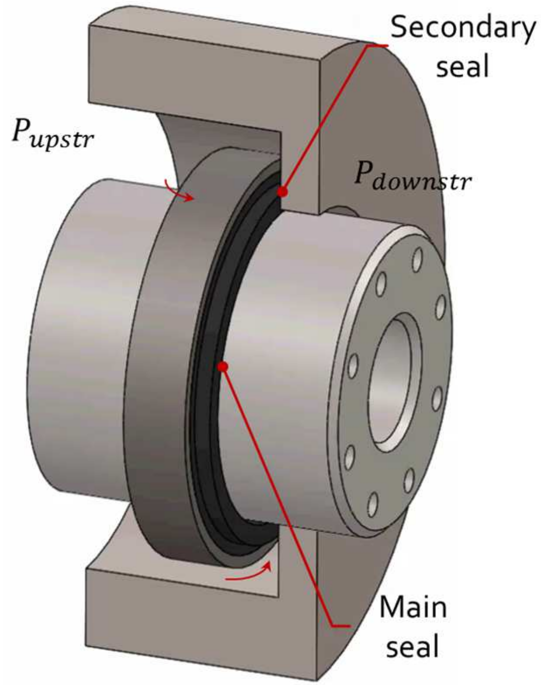

State of the art of the scientific literature

- R. G. Kirk and W. H. Miller, "The influence of high pressure oil seals on turbo-rotor stability," *ASLE transactions*, vol. 1, pp. 14-24, 1979.
- J. Semanate and L. San Andrés, "A quasi-static method for the calculation of lock-up speed in floating ring oil seals," in *Proc. of the 4th Congreso de Turbo-Maquinaria*, Querrettara, Mexico, 1993, pp. 55-62.
- S. Baheti and R. G. Kirk, "Thermo-hydrodynamic solution of floating ring seals for high pressure compressors using the finite element method," *STLE Tribology Transactions*, vol. 37, pp. 336-349, 1994.
- T. W. Ha, Y. B. Lee, and C. H. Kim, "Leakage and rotordynamics analysis of a high pressure floating ring seal in the turbopump unit of a liquid rocket engine," *Tribology International*, vol. 35, pp. 153-161, 2002.

- M. H. Nguyen, "Analyse des étanchéités annulaires à bague flottante" Poitiers, Thèse de doctorat 2011.
- M. Arghir, M. H. Nguyen, D. Tonon, and J. Dehouve, "Analytic Modeling of Floating Ring Annular Seals," *J. Eng. Gas Turbines and Power*, vol. 134, no. 5, 2012.
- M., Arghir, M.-H., Nguyen, “Non-Linear Analysis of Floating Ring Annular Seals: Stability and Impacts”, Proceedings of the 9th IFToMM International Conference on Rotor Dynamics, Milan, Italy, September 2014. DOI 10.1007/978-3-319-06590-8, pages 2007-2018.
- A. Mariot, "Analyse théorique et expérimentales des joints d’étanchéité à bague flottante et des joints rainurés segmentés " Poitiers, Thèse de doctorat 2015.
- A., Mariot, M., Arghir, P., Hélies, J., Dehouve, J., “Experimental Analysis of Floating Ring Annular Seals and Comparisons with Theoretical Predictions”, " *J. Eng. Gas Turbines and Power*, October 13, 2016, 138(4):042503-042503-9, doi: 10.1115/1.4031347.

- R. E. Burcham, "Liquid Rocket Engine Turbopump Rotating-Shaft Seals," NASA Lewis Research Center, Cleveland, Ohio, NASA SP-8121, 1978.
- R. E. Burcham, "High-speed crygoenic self-acting shaft seals for liquid rocket turbopumps," NASA Lewis Research Center, Cleveland, Ohio, NASA CR-168194, 1983.

Experimental analysis: first operating scenario

- The pressure difference ΔP across the floating ring increases with the rotation speed,
- For lower values of ΔP, the floating ring "follows" the rotor vibrations,
- As ΔP increases, the vibration amplitudes of the floating ring decrease because of the increasing friction forces on the nose,
- For high values of ΔP, the floating ring is "blocked" and acts as an eccentric annular seal,
- There is a possibility of contacts between the rotor and the carbon ring.

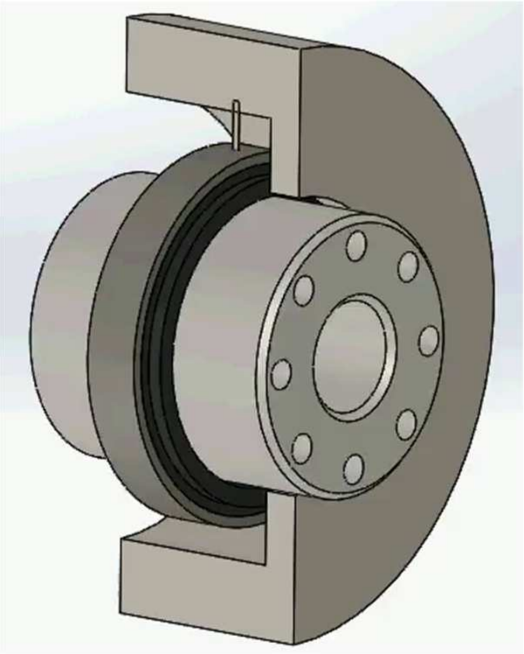

Experimental analysis: second operating scenario

- The pressure difference ΔP remains limited,
- The floating ring is not locked,
- The behavior of the floating ring can be periodic, quasi-periodic or chaotic.

There is still a possibility of contacts between the rotor and the carbon ring if the eccentricity is too high

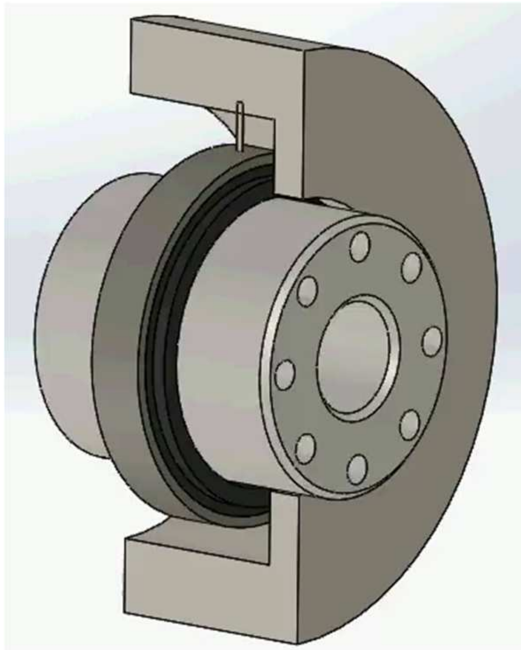

The test rig: FRAS in back to back arrangement

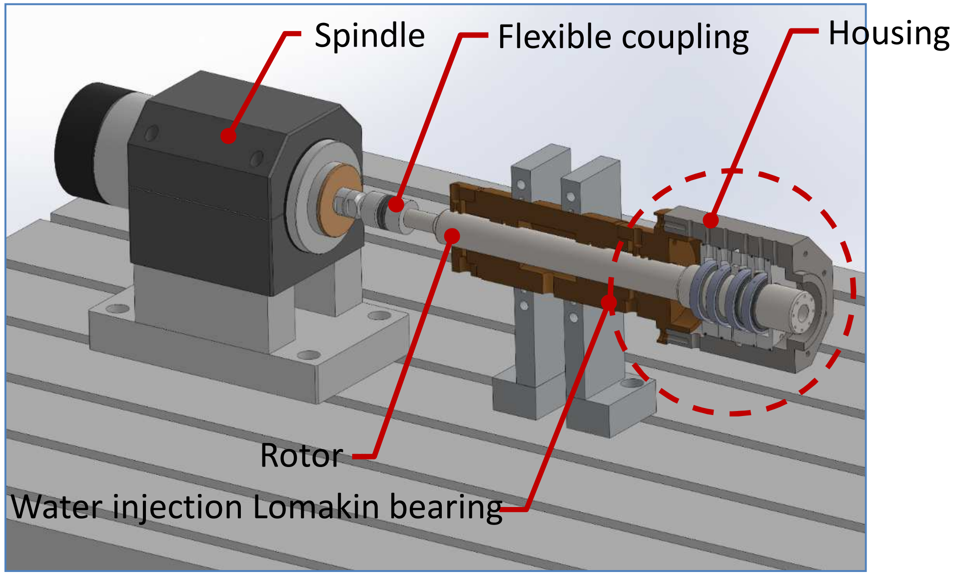

The test rig houses 2 to 4 floating ring seals in a back-to-back arrangement.

The displacements of the rotor and of the seals are measured in 6 positions along 2 orthogonal directions x, y.

The displacements are measured with inductive sensors.

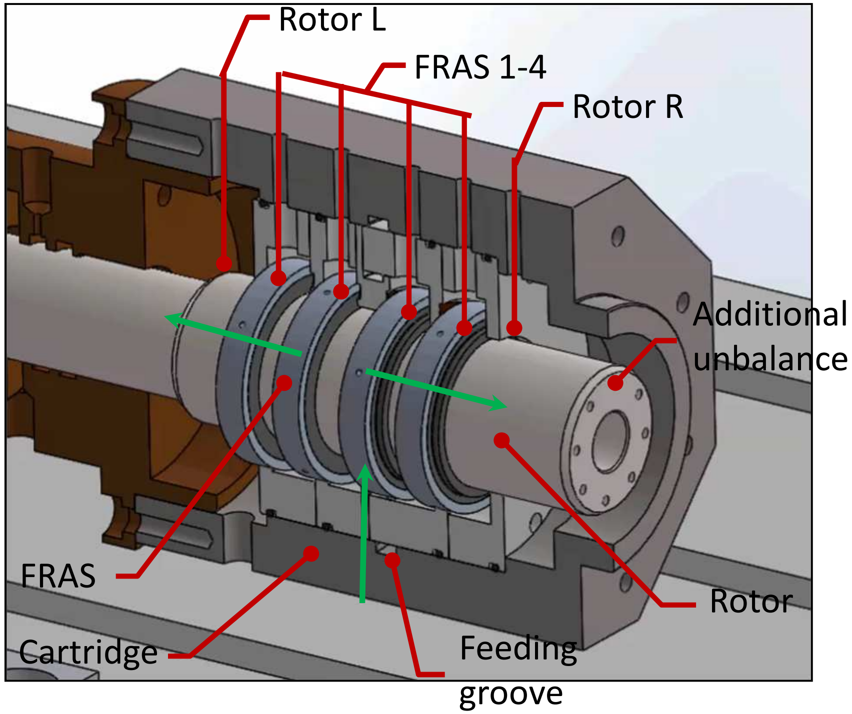

The rotation speed, feeding pressure and mass flow rate across the seal are measured.

Optical tracking of the FRAS

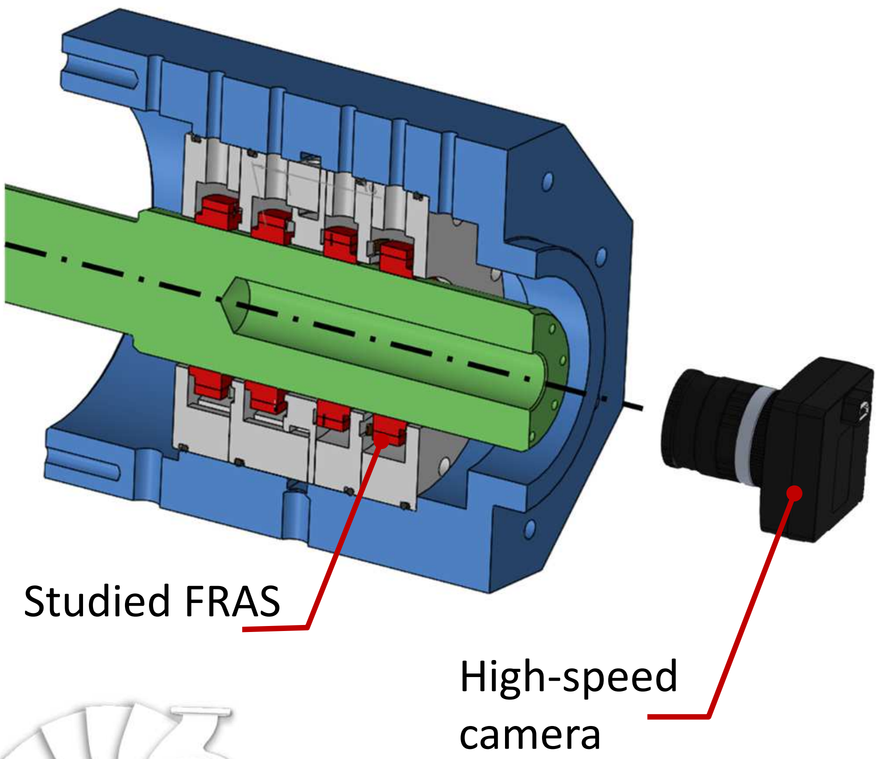

- A high-speed camera fitted with a high-magnification macro lens allows for observation of the radial clearance,
- It is possible to discriminate between centered and eccentric situations,
- A mark-tracking technique allows for measurement of the floating ring displacements,
- It is a backup solution for general use – only solution if the ring is not fitted with a steel collar.

Optical tracking of the FRAS

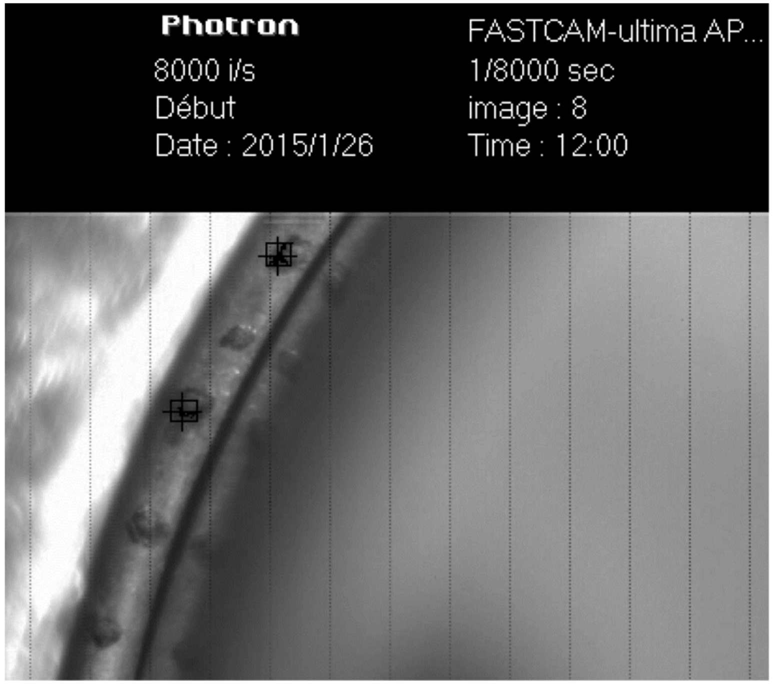

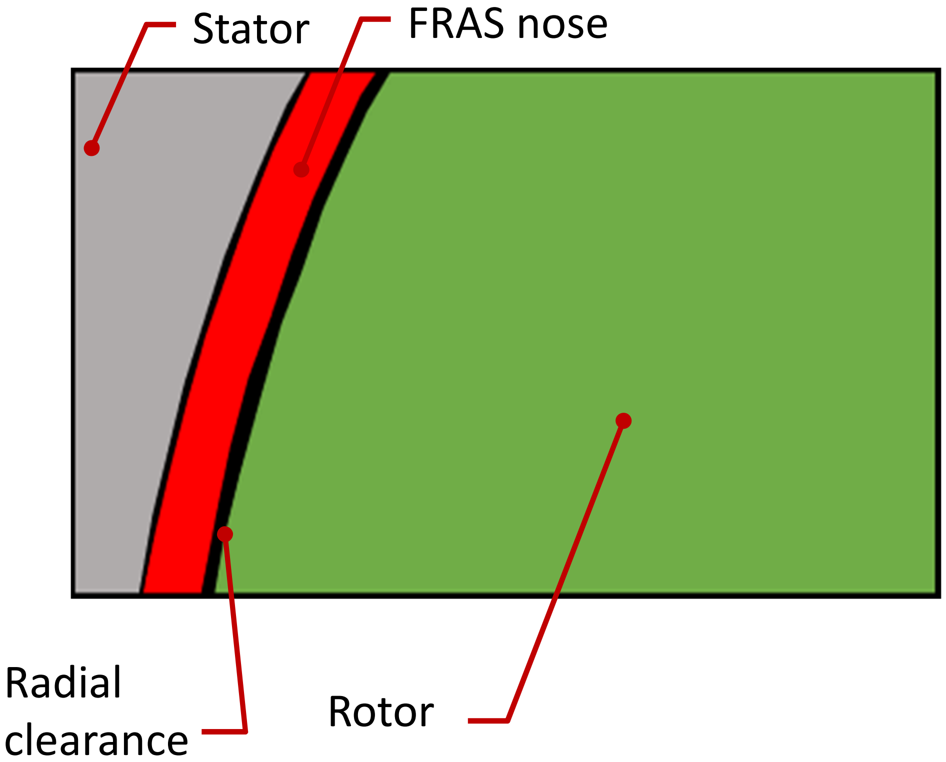

Geometry of the seals and of the rotor

Seals:

- 38 mm diameter seals, 10 mm axial length
- 4 different seals, divided in two categories:

– **Type 1** seals: small radial clearance (≈ 20 µm), low conicity (± 7 µm)

– **Type 2** seals: large radial clearance (≈ 30 µm), high conicity (± 15 µm)

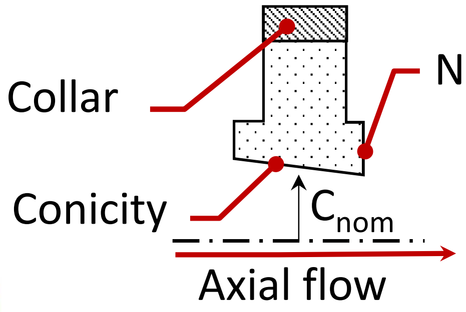

Rotor:

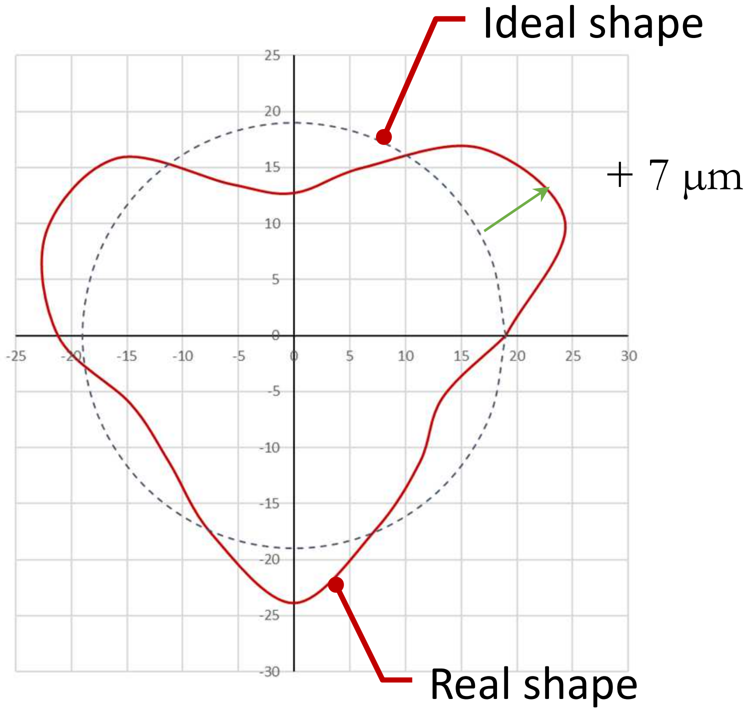

Experimental results: Ω=3000 rpm, ΔP=0.5 bar

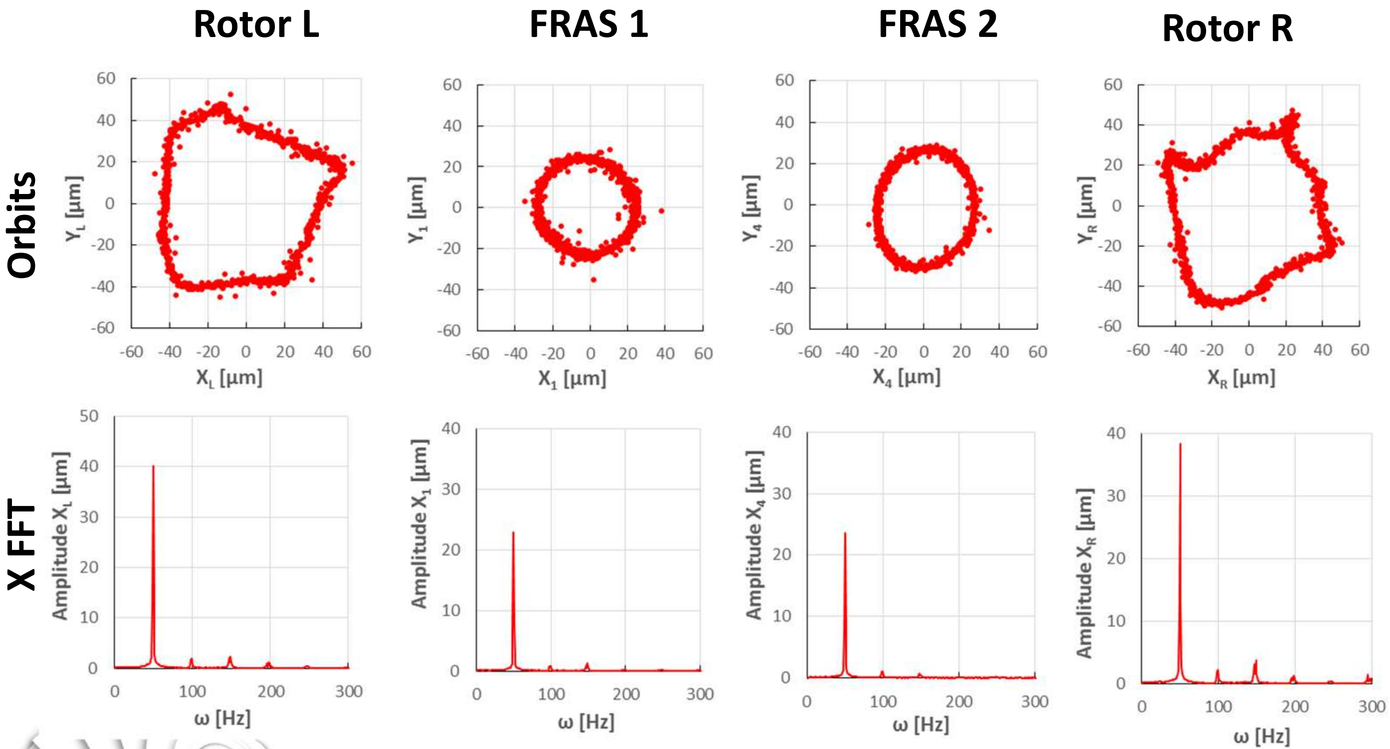

FRAS orbits are almost circular (2x and 3x spectral components are low compared to 1x)

The rotor 3x component is larger than the 2x due to runout errors

Remark: Y FFT are similar to X

Experimental results: Ω=3000 rpm, ΔP=1 bar

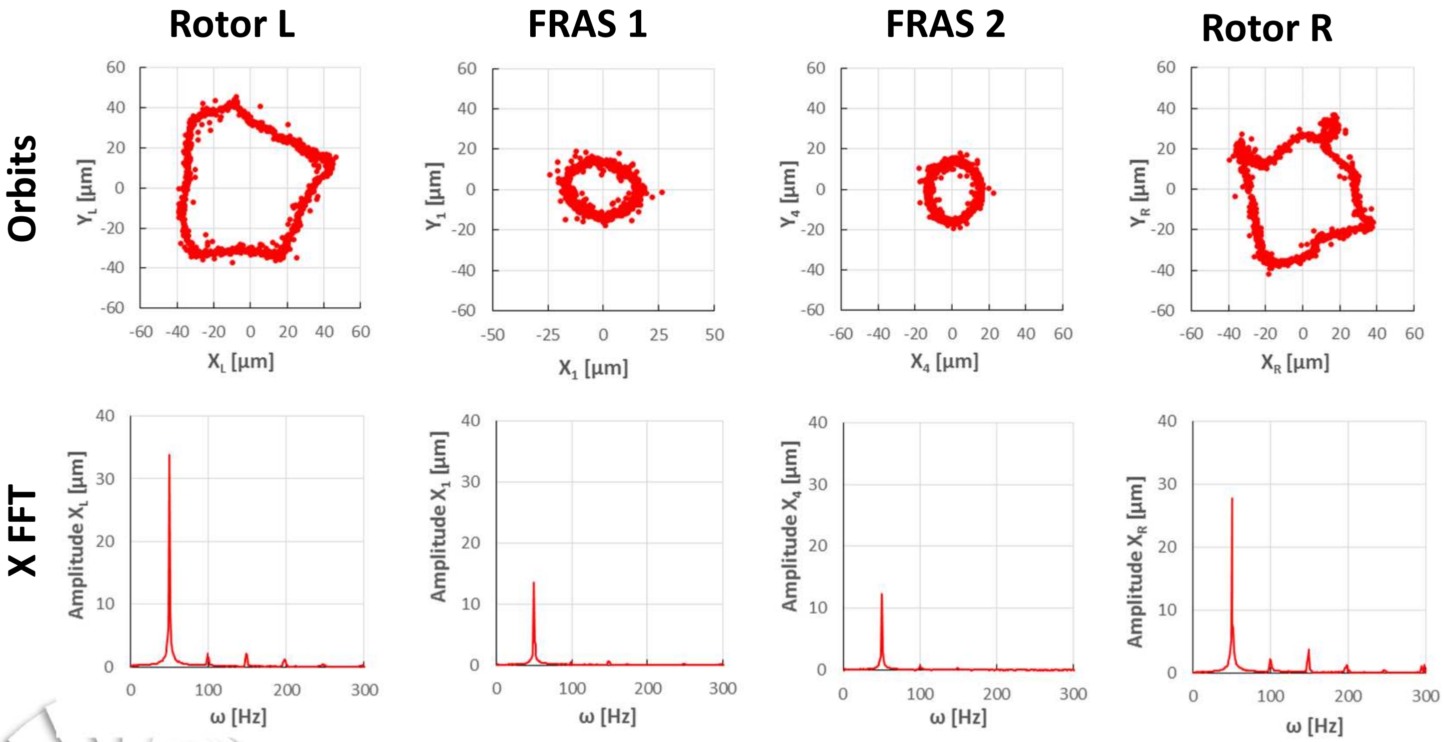

FRAS displacement amplitudes decrease with increasing ΔP

Remark: Y FFT are similar to X

Experimental results: Ω=3000 rpm, ΔP=1.5 bar

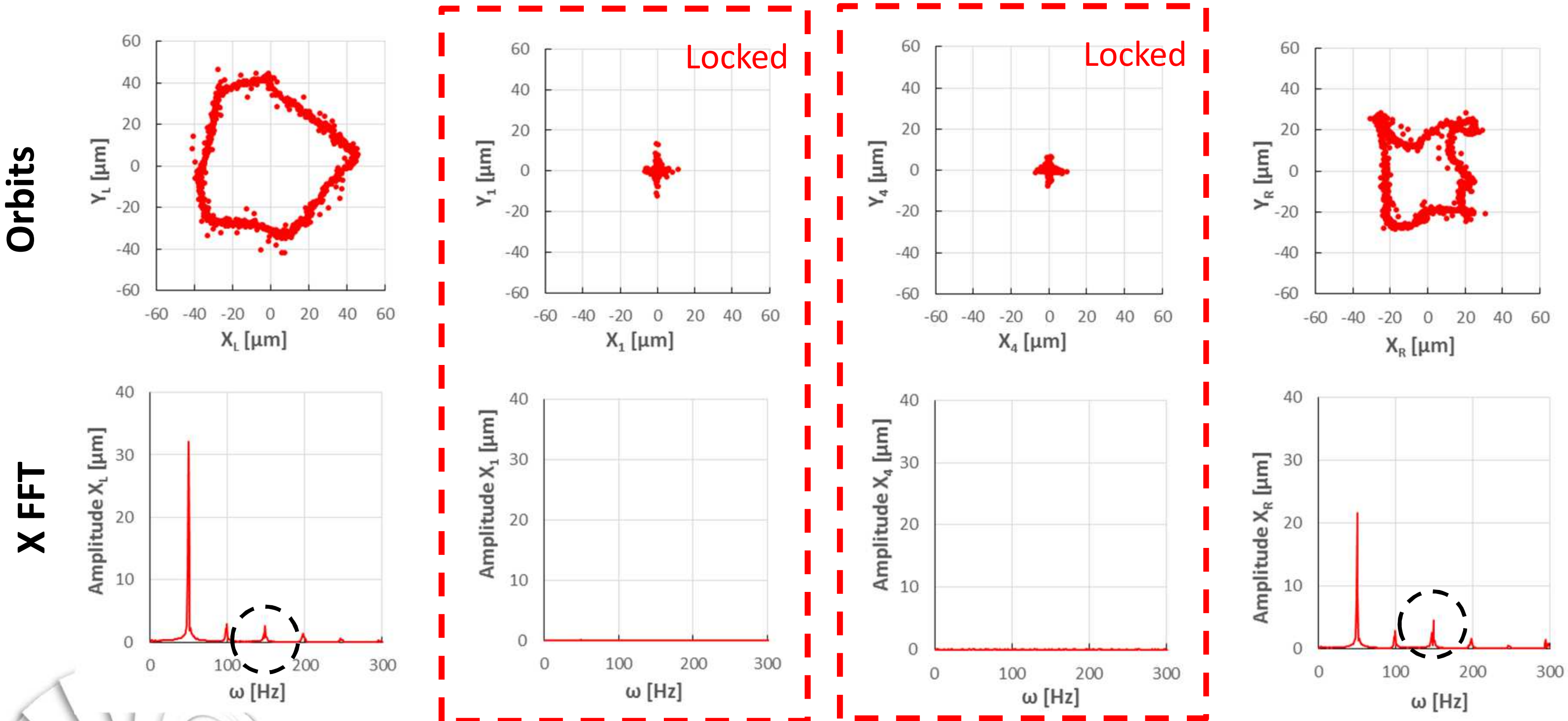

FRAS are locked!

Remark: Y FFT are similar to X

A numerical model for FRAS analysis

- The study is based on classical hydrodynamic lubrication theory,
- Both the rotor and the FRAS can move
  - Rotor displacements = input
  - FRAS displacements = output
- The trajectory of the FRAS is contained within a plane (no x, y-rotations),
- FRAS are fitted with anti-rotation pins: no z-rotation,
- Gravity effects are negligeable.

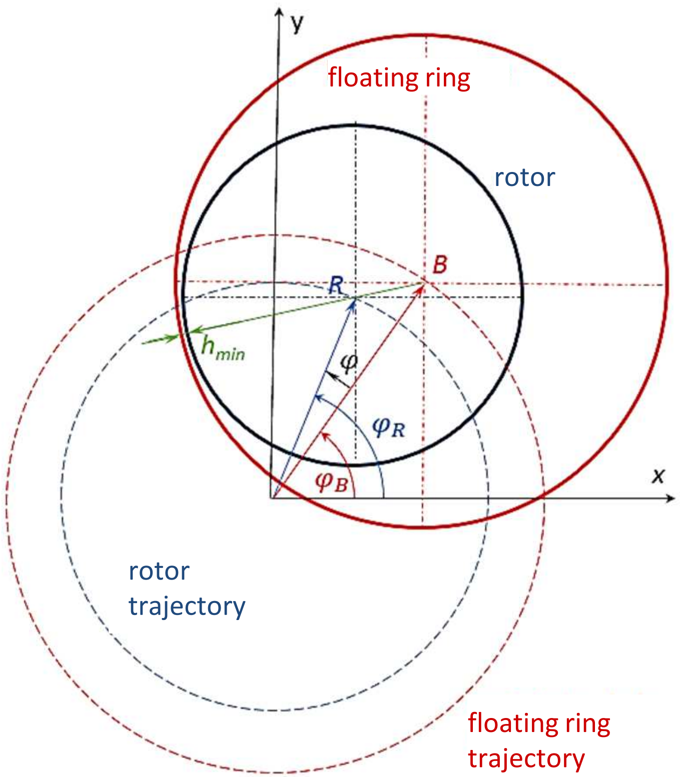

The equations of motion of the FRAS

- Forces on the floating ring:
  - Axial force F_z due to the pressure difference ΔP (compensated by the reaction force on the nose)
  - Hydrodynamic forces F_h in the main seal
  - Friction forces F_f on the nose of the FRAS
- Equations of motion:

$$m\begin{Bmatrix}\ddot{x}_B\\ \ddot{y}_B\end{Bmatrix}=\begin{Bmatrix}F_{h,x}\\ F_{h,y}\end{Bmatrix}+\begin{Bmatrix}F_{f,x}\\ F_{f,y}\end{Bmatrix}$$

Inertia forces

Hydrodynamic forces

Friction forces

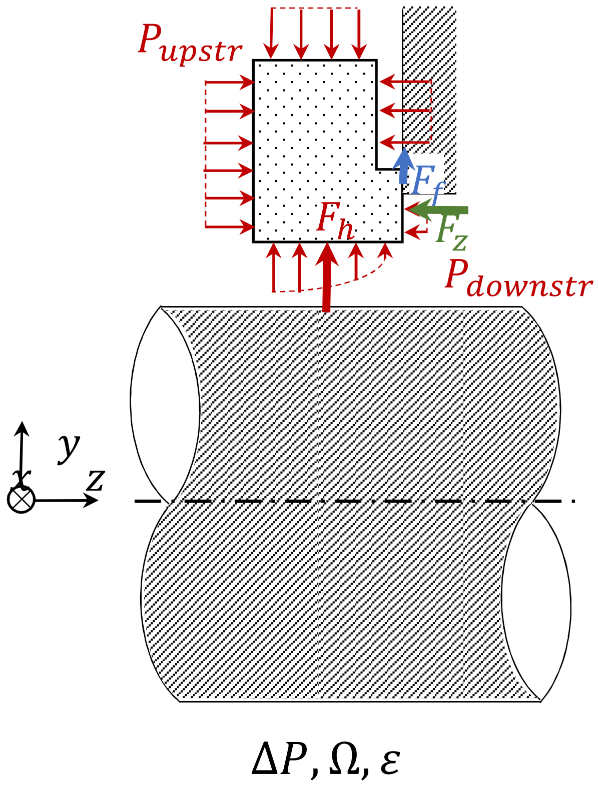

The hydrodynamic forces in the main seal of the FRAS

- The hydrodynamic forces in the main annular seal are expressed as the sum between static and damping contributions:

$$\begin{Bmatrix} F_{h,x} \\ F_{h,y} \end{Bmatrix} = \begin{Bmatrix} F_{h,x} \\ F_{h,y} \end{Bmatrix}_{(x_R - x_B, y_R - y_B, 0, 0)} - \begin{bmatrix} C_{xx} & C_{xy} \\ C_{yx} & C_{yy} \end{bmatrix} \begin{Bmatrix} \dot{x}_R - \dot{x}_B \\ \dot{y}_R - y_B \end{Bmatrix}$$

Static contribution Damping contribution

- The static forces and dynamic damping coefficients are computed by solving the zero and first order "bulk flow" equations

The computation of the static forces and dynamic damping coefficients is performed for a given seal geometry and pressure difference, rotation speed and eccentricity configuration.

Friction forces on the nose of the FRAS

- The secondary seal is not completely closed: a mixed lubrication regime subsists across the nose
- Normal forces on the floating ring:
  - Pressure difference $F_z = P_{amont}(R_3^2 - R_1^2) - P_{aval}(R_2^2 - R_1^2)$
  - Hydrostatic contribution $F_{z,fluide}$
  - Asperity contact forces $F_{z,asp}$
- Balance of forces:

$$F_z = F_{z,fluide} + F_{z,asp} \xrightarrow{\text{yields}} h$$

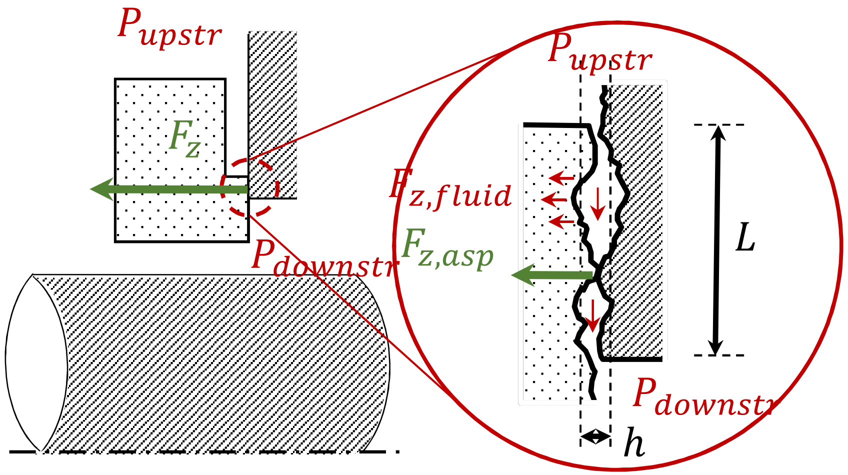

Contact forces: the contribution of asperities

Greenwood & Williamson's model for the contact between two rough surfaces:

- Contact between a nominally, rigid flat surface and a rough, deformable surface
- Asperities in contact are modelled as elastically loaded spheres of constant radius

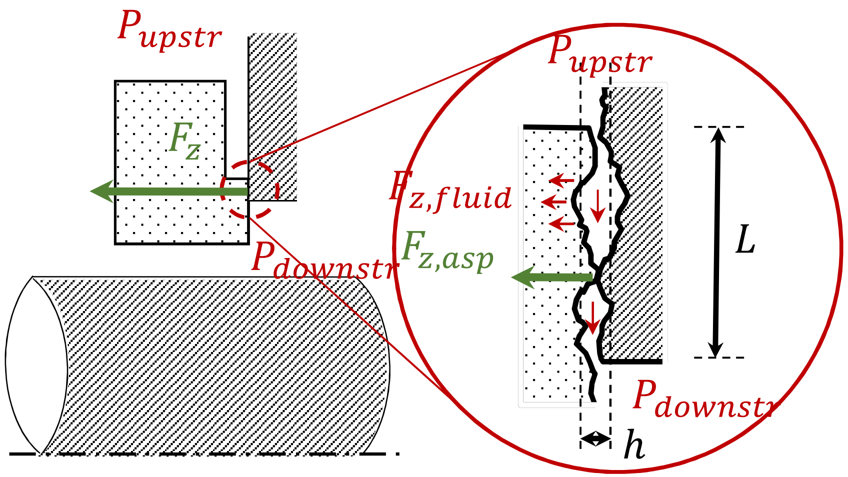

$$F_{z,asp} = \frac{4}{3} A_0 \eta E^* \sqrt{\beta} \int_h^{+\infty} (z_s - h)^{3/2} \varphi(z_s) dz_s$$

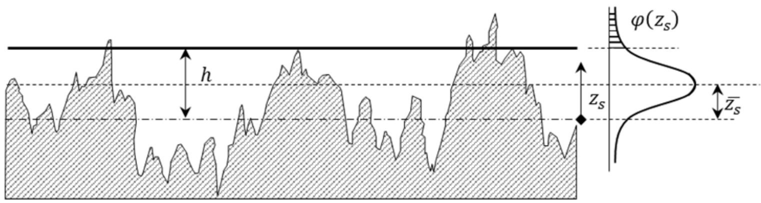

Contact forces: hydrostatic contribution

- The flow in the secondary seal is modeled as a 1D, adiabatic channel flow (height h, length L)
- The convective inertia effects are taken into account (bulk flow equations):

$$\frac{4f_f dz}{D_h} = \frac{(1-M^2)dM^2}{\kappa M^4\left(1+\frac{\kappa-1}{2}M^2\right)}$$

- The height of the canal is constant along the axial direction: analytic solution

$$\frac{2\bar{f}_f z}{h} = B(M_1) - B(M)$$

$$B(M) = \frac{1-M^2}{\kappa M^2} + \frac{\kappa+1}{2\kappa}\ln\left[\frac{(\kappa+1)M^2}{2+(\kappa-1)M^2}\right]$$

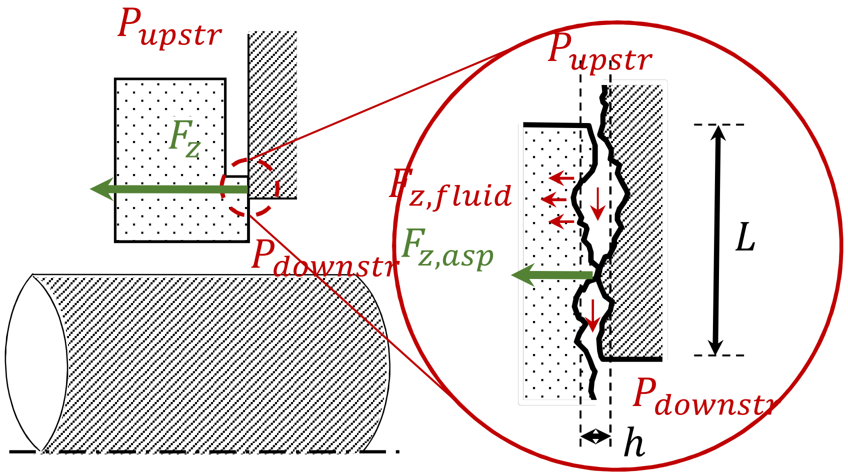

$$\frac{P}{P_1} = \frac{M_1}{M}\sqrt{\frac{1+\frac{(\kappa-1)M_1^2}{2}}{1+\frac{(\kappa-1)M^2}{2}}} \qquad \frac{T}{T_1} = \frac{1+\frac{(\kappa-1)M_1^2}{2}}{1+\frac{(\kappa-1)M^2}{2}}$$

The equivalent friction coefficient on the nose of the FRAS

- The relation between F_f and F_z can be expressed thanks to an "equivalent coefficient of friction" f_{eq}:

$$F_f = f_{eq} F_z$$

- Because of the hydrostatic contribution, the coefficient of friction f_{eq} is lower than the carbon/steel coefficient of friction
- f_{eq} depends on:
  - Surface conditions and geometry
  - Pressure difference

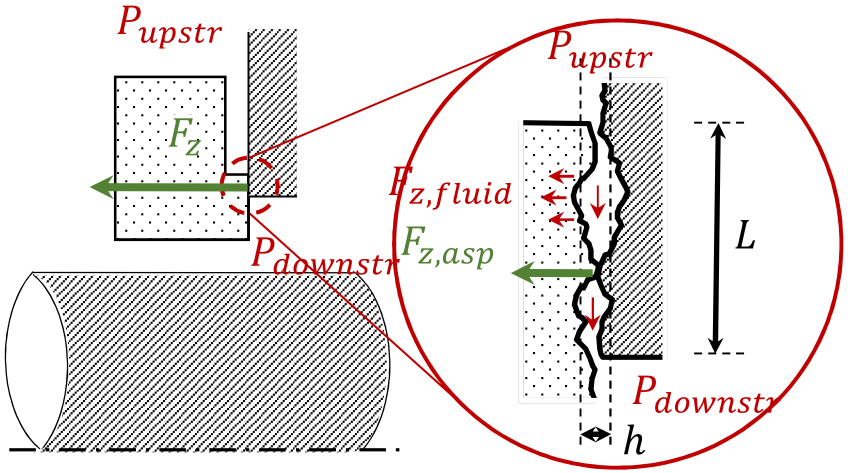

Comparisons experimental vs. theoretical trajectories

- The trajectories of the rotor show a high 3x spectral component due to rotor runout errors
- The rotor trajectory is corrected by eliminating spectral components higher than 2,5x
- Spectral components close to 2x are considered to be representative of the rotor trajectory (rotor misalignment and water bearing ovalization)

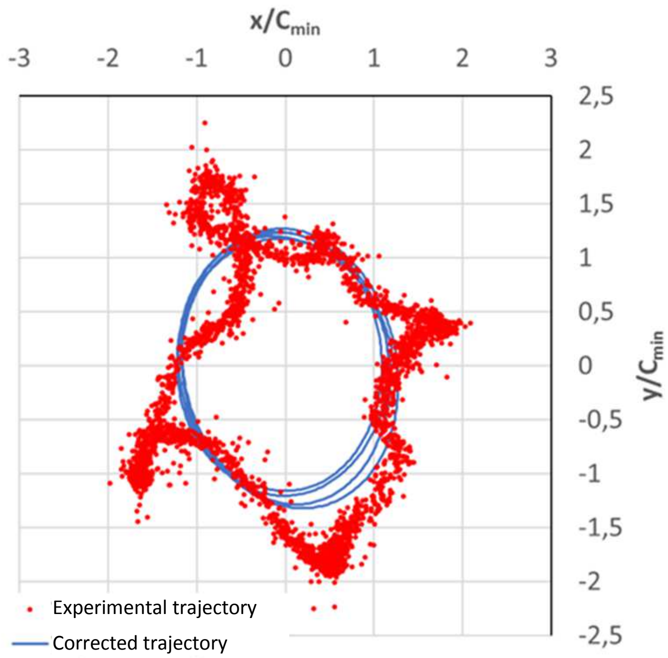

Case 1: FRAS#1, Ω=250 Hz, no additional unbalance

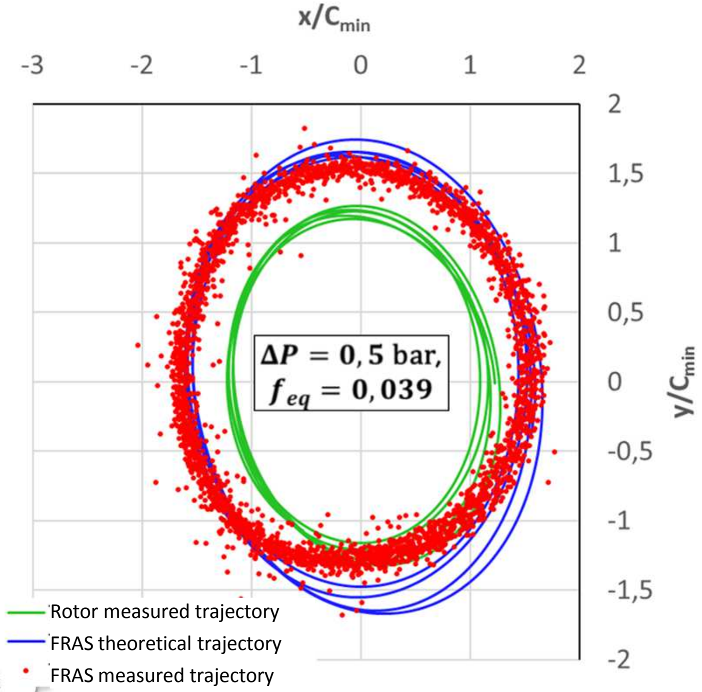

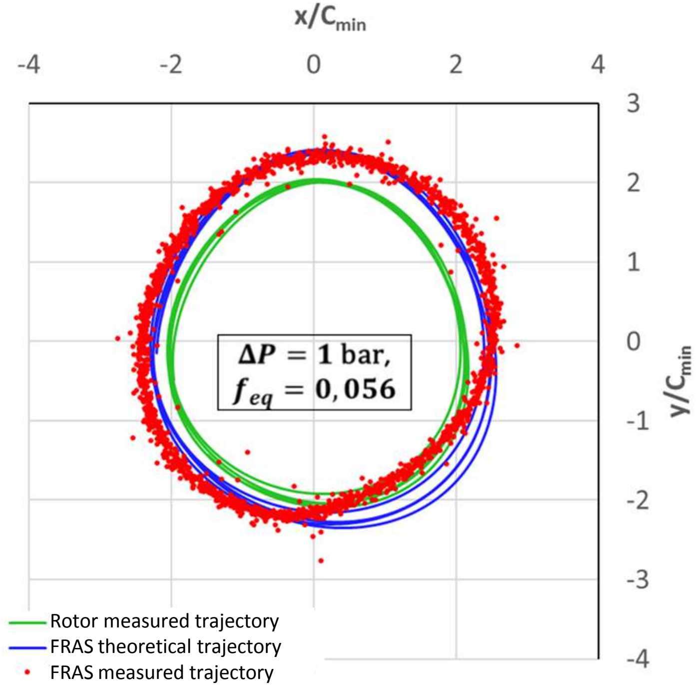

Case1: FRAS#1, Ω=250 Hz, no additional unbalance

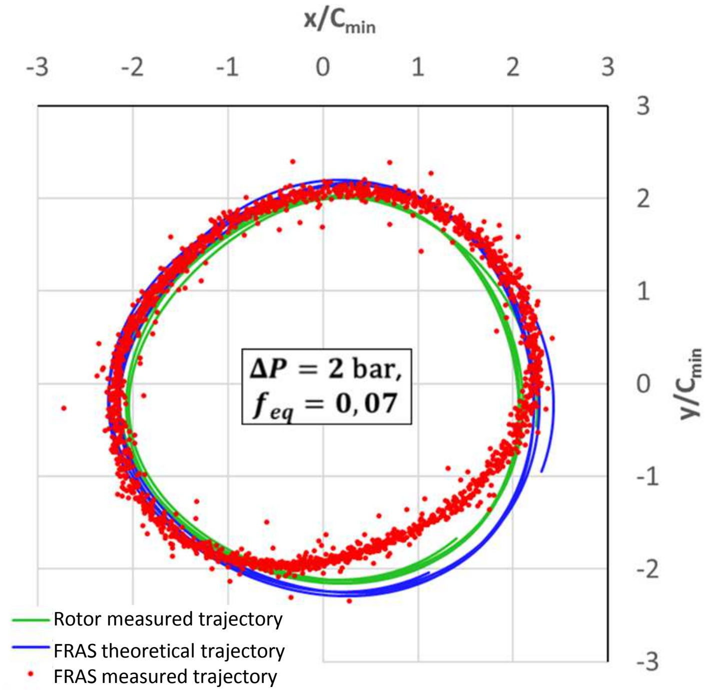

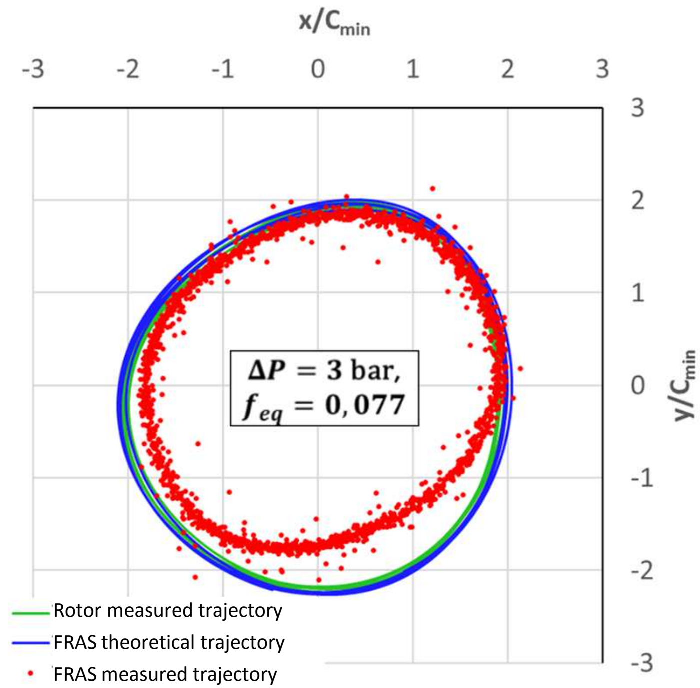

Results for FRAS#1, Ω=250 Hz, no additional unbalance

- The numerical model predicts closely the behavior of the seal
- The predicted eccentricity is $\approx 40\ \%$ and is constant with increasing ΔP (theoretical minimum film thickness is ≈ 8 µm)
- No predicted contact between the seal and the rotor
- The agreement between the predicted and experimental leakage rates accross the seal cartridge is good

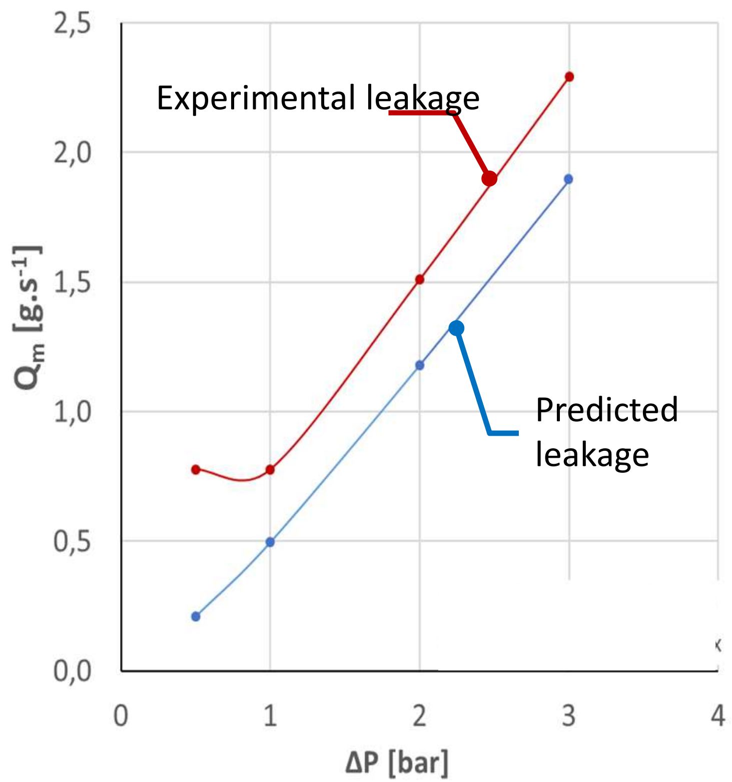

Case 2: FRAS#1, Ω=250 Hz, 25 g·mm additional unbalance

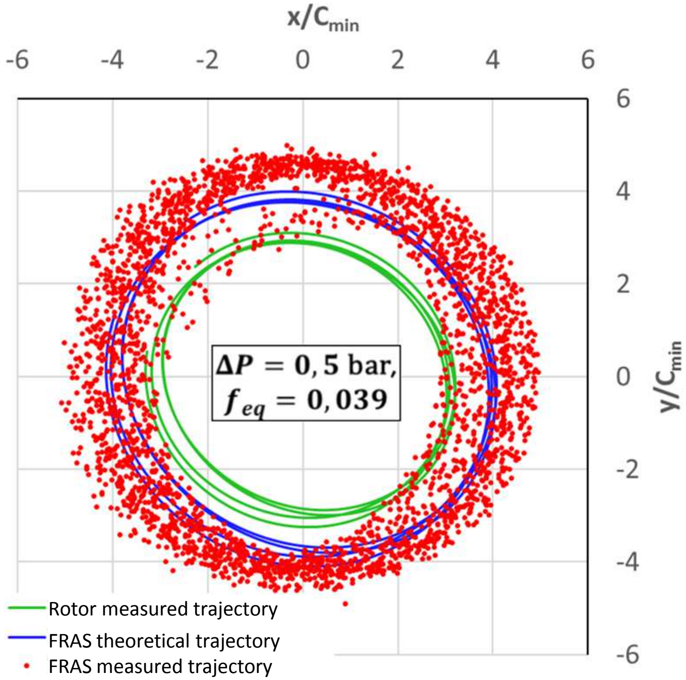

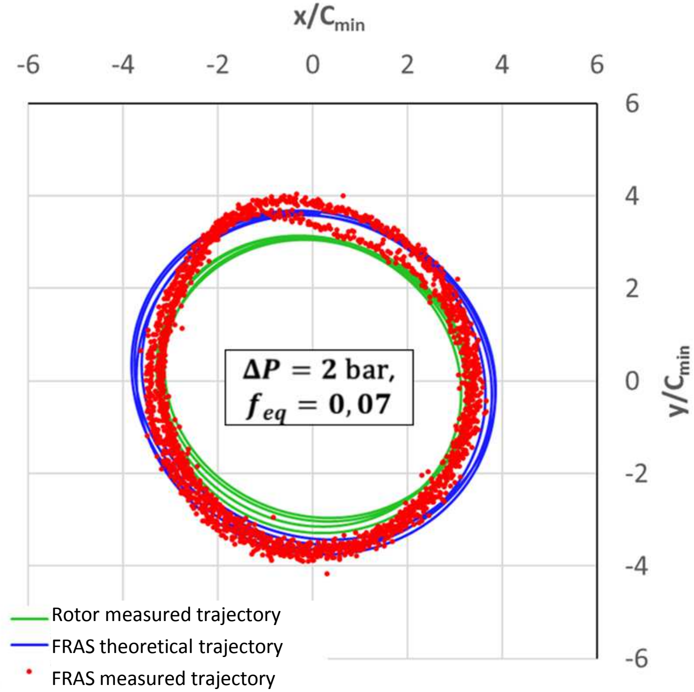

Case 2: FRAS#1, Ω=350 Hz, 25 g·mm additional unbalance

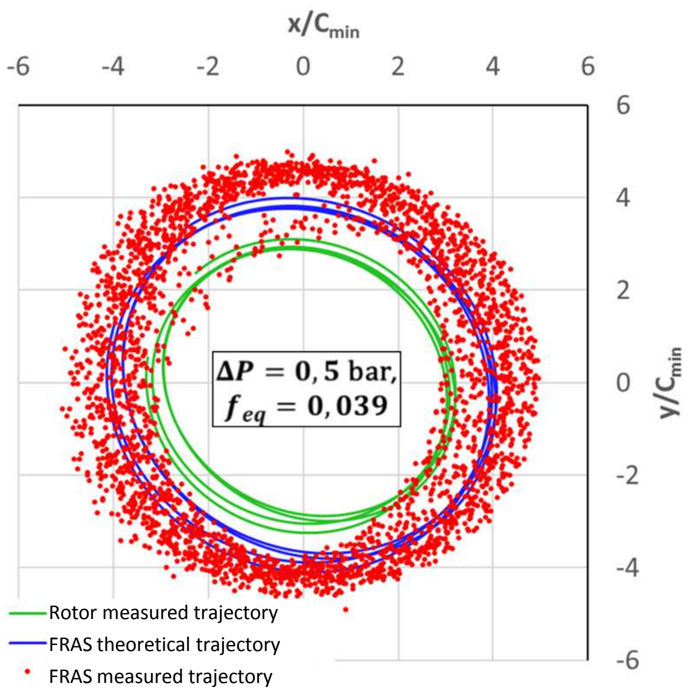

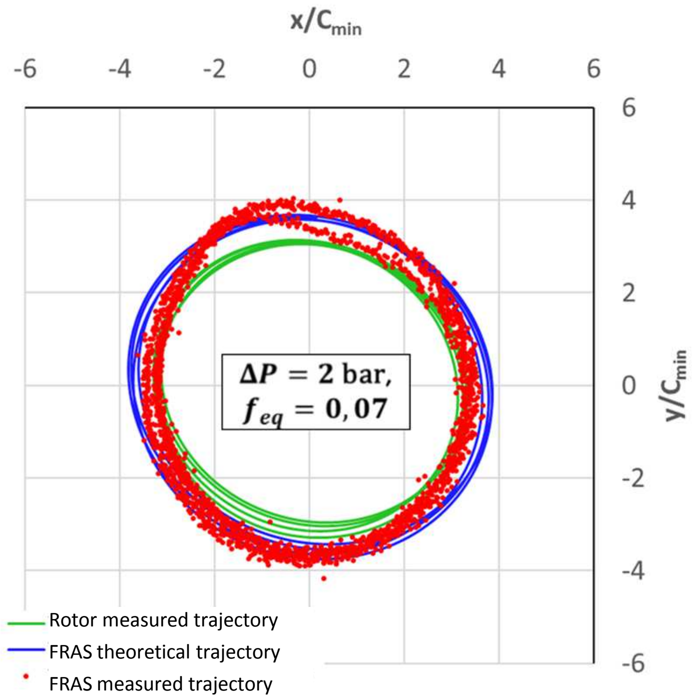

Case 2: FRAS#1, Ω=350 Hz, 25 g·mm additional unbalance

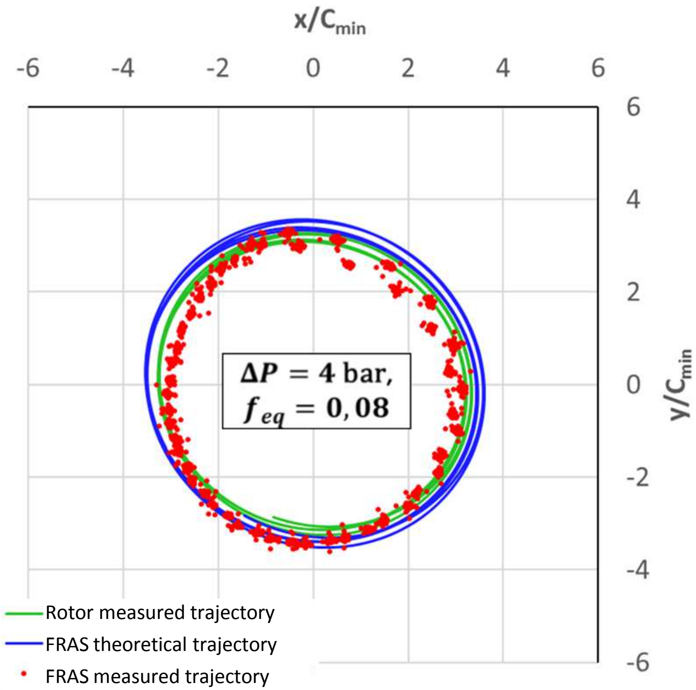

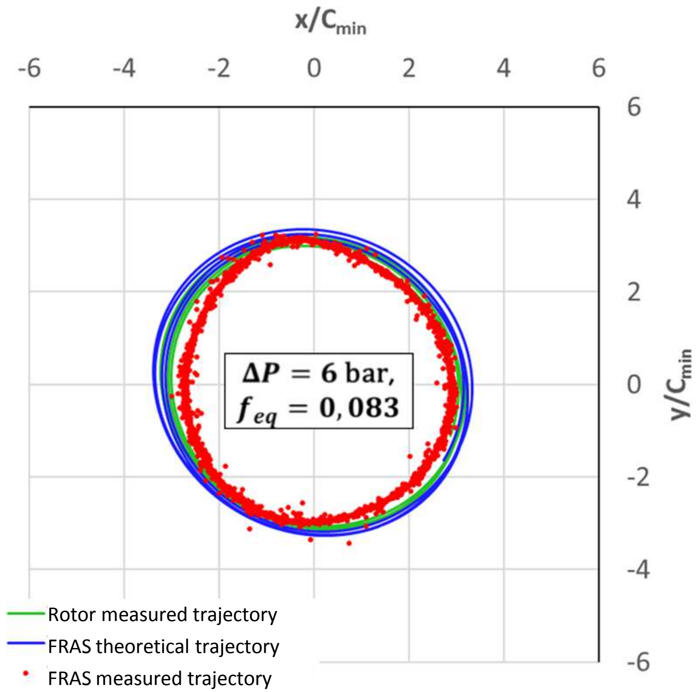

Case 2: FRAS#1, Ω=350 Hz, 25 g·mm additional unbalance

- Again, the numerical model predicts closely the behavior of the seal
- The predicted eccentricity varies between 40 and $70\ \%$ and **decreases** with increasing ΔP (predicted minimum film thickness is 0 to $10\ \mu\text{m}$)
- Possibility of contacts even though the seal is not locked
- The agreement between the predicted and experimental leakage rates accross the seal cartridge is good

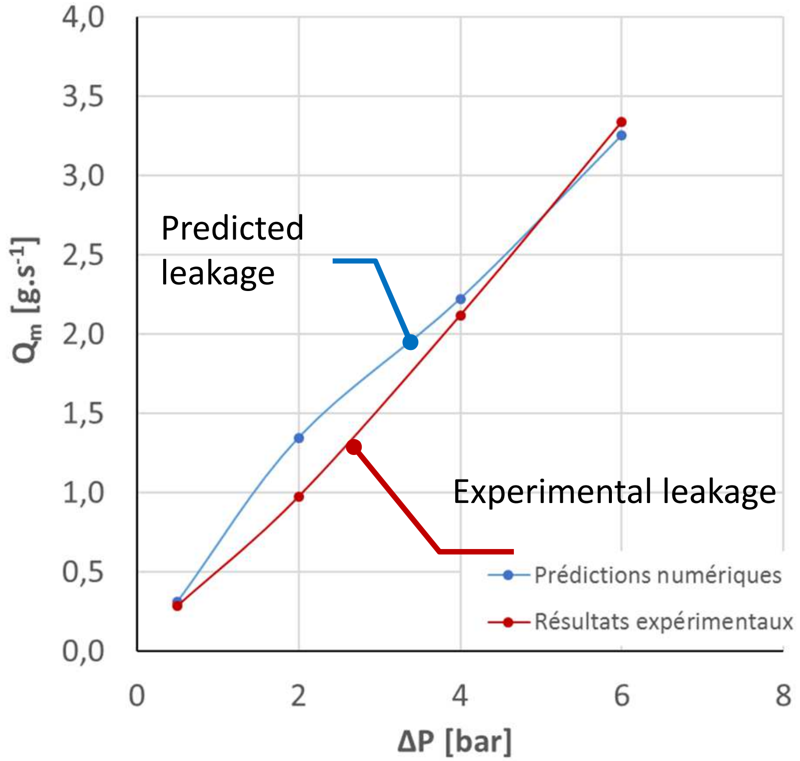

Case 3: FRAS#2,no additional unbalance

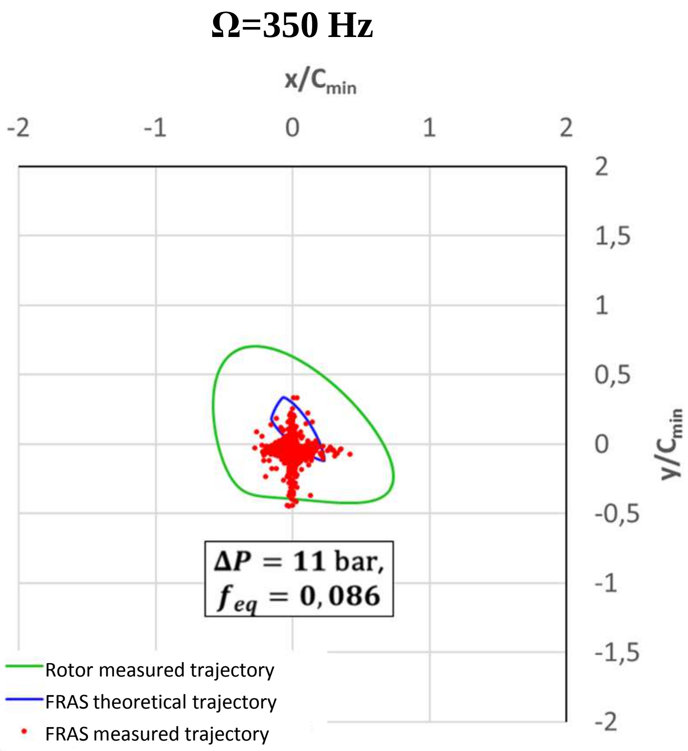

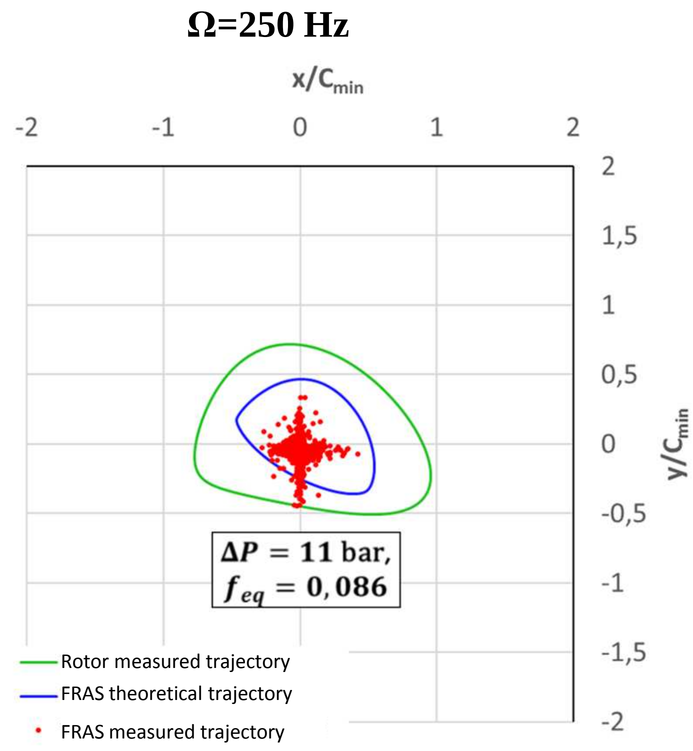

Conclusions

- The predicted behavior of the FRAS (locked/unlocked) depends on a combination of ΔP, Ω and rotor excitation amplitudes,

- The two scenarios were experimentaly and numericaly reproduced:
  - for a low ΔP and large enough rotor vibrations, the FRAS follows the rotor
  - if the ΔP increases OR if the rotor vibrations are too low, the FRAS is progressively locked

- FRAS follows the rotor $\neq$ centered,
- For a low ΔP, the eccentricity may be high enough to cause rotor/seal contacts,
- Moving FRAS = more damage than locked one!
- The impact of FRAS (locked or not) on the rotor dynamic behavior has to be considered.

ASIA TURBOMACHINERY & PUMP SYMPOSIUM
MARCH 2018 | SUNTEC SINGAPORE

Thank you!

Questions?

TURBOMACHINERY LABORATORY
TEXAS A&M ENGINEERING EXPERIMENT STATION

TEXAS A&M UNIVERSITY